Selective Crystallization of Metastable α-Form of L- glutamic Acid through Feedback Concentration Control

Nicholas C. S. Kee[†,§,‡], Reginald B. H. Tan[§,‡] and Richard D. Braatz[†]

[†] University of Illinois at Urbana-Champaign, Illinois, USA;
[§] National University of Singapore, Singapore;
[‡] Institute of Chemical and Engineering Sciences, Singapore

Introduction

Polymorphism is described as the ability of a compound to adopt different crystalline arrangements.[1] Although chemically identical, different polymorphic structures display a variation in its physical properties such as crystal morphology, density, solubility, and color. These in turn exert an influence on the performance of the product; for example, the bioavailability and shelf-life of pharmaceutical compounds. It is pertinent to have a consistent and reliable production process for the desired polymorph to achieve feasible economic yield and for compliance of regulatory aspects. The thermodynamically stable polymorph can be obtained without much complication as long as sufficient process time is allowed under suitable crystallization conditions like temperature and stirring rate. The metastable form is more difficult to obtain; the main challenge being to prevent its transformation. L-glutamic acid in water was chosen as the model system. L-glutamic crystals have two known polymorphs; forms α and β which are monotropically related.[2] The β-form consists of needlelike platelets (Figure 1a), while the α-form has a prismatic morphology (Figure 1b). At 45°C or higher, excess amounts of α-form L-glutamic acid in a saturated aqueous solution will transform into the stable β form; this transformation is solvent-mediated and consists of two steps, the dissolution of the α crystals and the re-nucleation and growth of the β-form.[2,3,4]
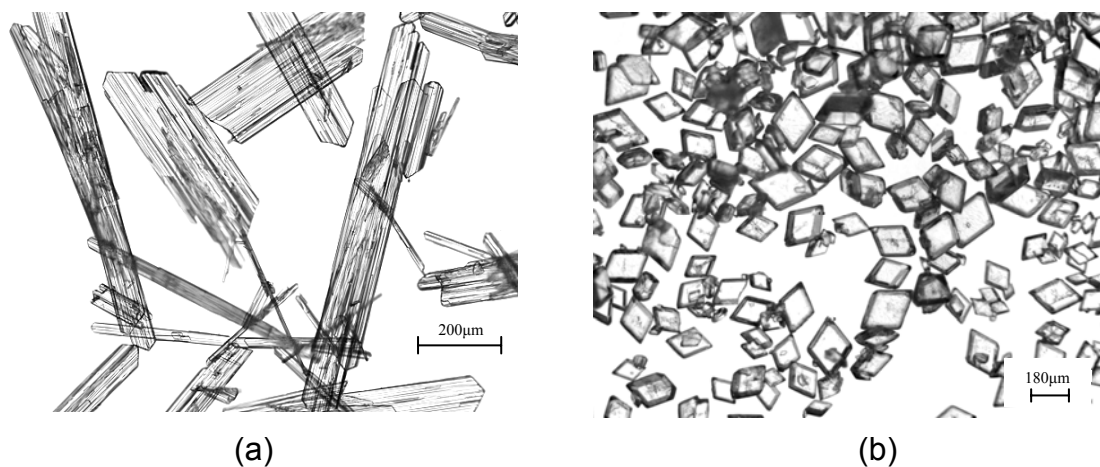
Figure 1. Microscopy images of L-glutamic acid crystals: (a) β-form, (b) α-form.

Industrial batch crystallization processes are typically designed to follow an optimal temperature or solvent addition profile, which derivation necessitates accurate nucleation and crystal growth kinetics or trial-and-error experimentation. The kinetic information can be obtained from a succession of crystallization experiments,[5,6] but this may prove laborious and time-consuming for complex systems. A different approach, which does not require accurate kinetic data or repetitive trials, is to operate the crystallizer based on the solution concentration measurement so that it follows a supersaturation profile within the metastable zone to avoid unwanted nucleation.[7,8,9] An advantage of this concentration control strategy is its robustness against variation in growth or nucleation kinetics and practical disturbances, and has been demonstrated for both cooling and antisolvent crystallizations in non-polymorphic systems.[10,11]

This paper describes the application of this concentration control methodology for the polymorphic system of L-glutamic acid in water. The objective is to achieve selective crystallization with uniform crystal size of the metastable polymorph for a seeded system. The lower and upper bounds of the operating regime are specified by the α-form solubility curve and metastable limit, respectively. ATR-FTIR (attenuated total reflectance-Fourier transform infrared) spectroscopy coupled with a calibration model constructed using chemometrics techniques[12,13] was used to provide in-situ solution concentration measurement. FBRM (focused beam reflectance measurement), which measures in-situ the characteristics of crystal size distribution, was used to detect the metastable limit, as previously demonstrated[10,14,15] for the seeded system. The seeded batch cooling crystallizations are implemented with the feedback concentration control approach using different supersaturation profiles to obtain the most appropriate batch crystallization recipe for selectively growing metastable L-glutamic acid crystals.

Experimental Procedures

Materials and Instruments

A Dipper-210 ATR immersion probe (Axiom Analytical) with ZnSe as the internal reflectance element attached to a Nicolet Protégé 460 FTIR spectrophotometer was used to obtain the aqueous L-glutamic acid spectra. The chord length distribution of L-glutamic crystals in solution was measured using Lasentec FBRM. The solution temperature was controlled by rationing hot and cold water to the jacket with a control valve as described previously.[16,17] The X-ray diffraction (XRD) patterns of the L-glutamic acid crystals were collected offline based on powdered samples, using Bruker General Area Detector Diffraction System (GADDS, Bruker AXS, Inc.) with Cu $K_{\alpha1}$ and Cu $K_{\alpha2}$ (weighted sum) radiation and a step size of 0.02°. The polymorphic composition was calculated using a convolution based profile fitting algorithm[18] available in the Diffracplus Topas (version 3.0, AXS Bruker Inc.) software, based on the crystallographic information (lattice parameters and atomic coordinates).[19,20] The L-glutamic acid crystals obtained commercially (99%, Sigma Aldrich) were verified using XRD to be β crystals (>99.89% β-form). α L-glutamic acid crystals were obtained using a rapid cooling method, outlined previously,[3,4] and the purity was verified similarly using XRD (>99.52% α-form).

Calibration for Solution Concentration

Different solution concentrations of L-glutamic acid (99%, Sigma Aldrich) and degassed deionized water were placed in a 500-ml jacketed round-bottom flask and heated until all the crystals dissolved. The solution was cooled at 0.5 $^{\circ}$C/min, while the IR spectra were being collected. The IR spectra of aqueous L-glutamic acid in the range 1100–1450 cm^{-1} were used to construct the calibration model. The calibration model relating the IR spectra and temperature to solution concentration was determined as described previously using various chemometrics methods such as principal component regression and partial least square regression (PLS).[21] The chemometrics forward selection PCR 2 (FPCR 2) method[22] was selected because it gave the smallest prediction interval; using a noise level of 0.001, the prediction interval (0.73 g/kg) was compatible with the accuracy of this model with respect to available solubility data.[3]

Solubility and Metastable Limit Measurements

For each polymorph, the IR spectra of L-glutamic acid slurries (saturated, and with excess crystals) were collected at different temperatures ranging from 25°C to 60°C. The slurry was equilibrated for 45 minutes to an hour at a specified temperature before recording the IR spectra. The solution concentration was then calculated using the aforementioned calibration model. The metastable limit of L-glutamic solutions was determined at various solution concentrations, using the polythermal method.[23] Each solution was heated to 5°C above its saturation temperature and maintained at 1 hour, before being cooled at a fixed rate of 0.4 °C/min. The chord length distribution of the crystals was monitored using FBRM. As the main crystallization experiments utilized seeding, the metastable limit was determined for the seeded system; α crystals (0.23 g, 90-250 μm) were added at 2°C after the solution temperature crossed the α-form saturation temperature. The start of sharp increase in the total counts after seeding was considered to be the onset of secondary nucleation at the metastable limit.

Seeded Batch Crystallization

Appropriate amounts of L-glutamic acid in 400 g of water was heated to an initial temperature 55°C (5°C above the β-form saturation temperature) in a 500-mL jacketed round bottom flask with an overhead mixer at 250 rpm, to create an undersaturated solution at a solution concentration of 20 g/kg. The crystallizer was then cooled at 0.4 °C/min to 39.5°C (2°C below the α-form saturation temperature), upon which α seed crystals (0.23 g, 90-250 μm sieve fraction, shown in Figure 1b) were added. The seed mass represented a seed loading ratio of approximately 0.09. Supersaturation setpoint profiles were followed during crystallization based on in-situ solution concentration measurement as described previously.[10,11] The control algorithm was started shortly after seeding. Supersaturation setpoint profiles were selected at different constant absolute supersaturation ($\Delta C = C - C_{sat}$) and constant relative supersaturation ($\Delta C_r = \Delta C / C_{sat}$) with respect to the α-form, where C is the solution concentration and C_{sat} is the solubility. A similar run was carried out at $\Delta C = 3.2$ g/kg but at a higher initial solution concentration (28 g/kg) with correspondingly higher initial and seeding temperature, 65°C and 48.3°C respectively.

Results and Discussion

Solubility and Metastable Limit Measurements

Figure 3 plots the solubility curves of both α and β-forms of L-glutamic acid. There is good agreement with previous experimental data.[3] The average errors for the α-form and β-form solubility curves are 0.27 g/kg and 0.39 g/kg, respectively, while the maximum errors amounted to 0.51 g/kg and 0.69 g/kg, respectively. These were within the computed prediction intervals of the calibration model. To determine the metastable limit of the seeded system, a fixed cooling rate of 0.4 °C/min was chosen because this cooling rate was sufficiently fast to cool an initially undersaturated solution (region 1 in Figure 4) across both solubility curves (into region 3) to achieve supersaturation with respect to the α-form, without any undesired nucleation of β-form crystals. This provided a window to seed and grow α crystals in a controlled manner. Further cooling (into region 4) would increase the driving force to grow the seed crystals but there will be uncontrolled secondary nucleation once the metastable limit is crossed. Thus, the seeded metastable limit provides an estimate of the maximum allowable supersaturation for the controlled growth of α-form seed crystals. Using lower cooling rates than 0.4 °C/min led to primary nucleation before the solution significantly entered region 3 and could be seeded with α-form crystals. This form of nucleation occurred either in region 2 or very close to the α solubility curve in region 3. The unintended primary nucleation is detrimental to the selective and controlled growth of the α seed crystals in terms of the product crystal size distribution and purity.
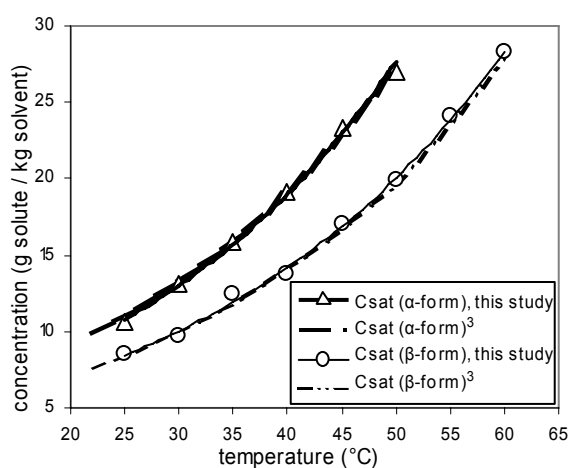
Figure 3. Solubility curves for α and β-form L-glutamic in water.
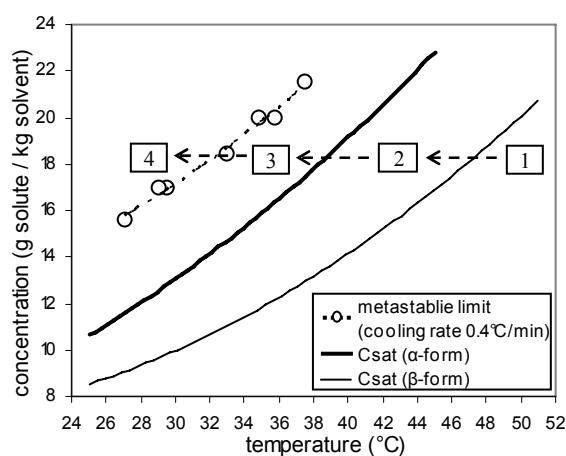
Figure 4. Metastable limit and solubility curves of L-glutamic acid solution.

Concentration-Controlled Batch Crystallization

Figure 5 shows the supersaturation profile of the seeded concentration-controlled crystallization carried out with the higher solution concentration (and seeding temperature) at ΔC = 3.2 g/kg. The operating temperature range upon seeding was from 48.3°C to 39°C. Needle-shaped β crystals are observed on the surfaces of α-forms in the crystal produced from this run (Figure 6). This is consistent with previous reports on the surface nucleation of β L-

glutamic acid crystals.[24,25] Compositional analysis based on XRD verified the polymorphic contamination (92.45% α-form, 7.55% β-form).
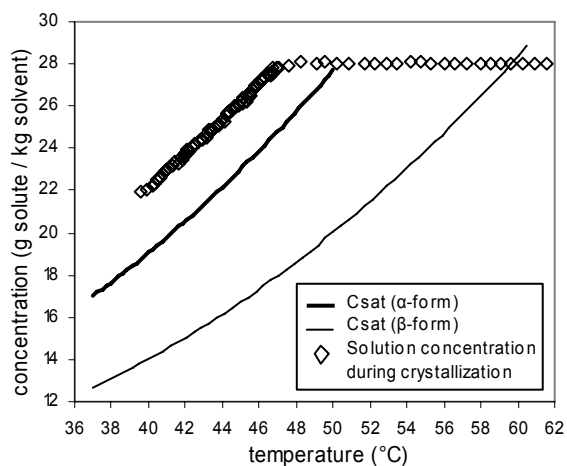
Figure 5. Supersaturation profile followed during the seeded batch crystallization experiment.
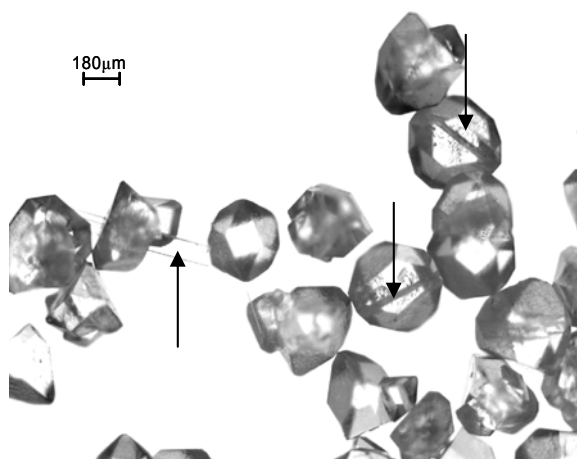
Figure 6. Microscopy image of L-glutamic acid product crystals. β-form is indicated by an arrow.
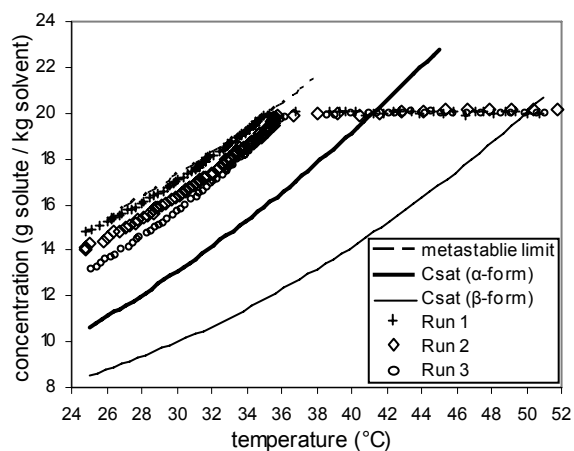
Figure 7. Supersaturation profiles followed during the seeded batch crystallization experiments.
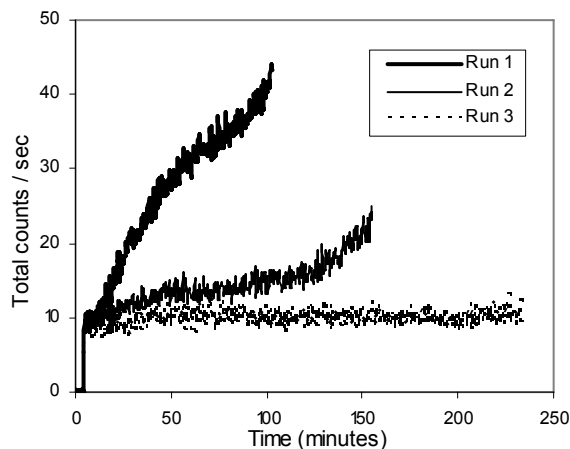
Figure 8. Total counts / sec profiles in the seeded batch crystallization experiments.

To avoid the nucleation and growth of β crystals, a lower temperature range (39.5°C to 25°C) was used for seeding and crystal growth for the following three runs. Figure 7 shows the different supersaturation profiles implemented in the seeded crystallization experiments. Runs 1 and 2 were carried out with ΔC at 4.2 g/kg and 3.2 g/kg, respectively. Run 3 was implemented with a relative supersaturation ΔC_r = 0.212. The supersaturation profiles for Runs 2 and 3 remained in the metastable limit throughout the run, while that of Run 1 crossed it initially and stayed very close to the metastable limit for the remainder of the run.

The impact of using different supersaturation profiles are observed from the FBRM particle count profiles (Figure 8); in Run 1, the particle counts increased at the initial stages due to secondary nucleation which occurred when the supersaturation profile crossed the metastable limit. For Run 2, the particle counts remained nearly constant except for a slight increase towards the end of the run. The increase in the particle counts in the late stages of Run 2 is consistent with earlier findings that secondary nucleation tends to increase with increased crystal mass.[26] This explains the increasing secondary nucleation as the crystallization proceeds at constant absolute supersaturation. Maintaining a constant relative supersaturation (decreasing absolute supersaturation) in Run 3 compensated the effect of increasing crystal mass to effectively reduce excessive secondary nucleation.

Figure 9 shows the crystals produced from Run 2 and Run 3, which had little or no secondary nucleation. The morphological change (from rhomboid to hexagonal with increase in the thickness of the crystal) is consistent with earlier reports of α-form growth.[27] The crystals are of fairly uniform size (240-510 μm), as opposed to that of Run 1 which had significant secondary nucleation. The product crystals of Run 1 were of varying sizes and agglomeration was also observed (Figure 10). The XRD analysis of the product crystals from Runs 1-3 indicated negligible amounts of β crystals in the product. For this temperature range and seeding conditions, the secondary nucleation which occurred at the metastable limit in Run 1 produced α crystals only.

(a)   (b)
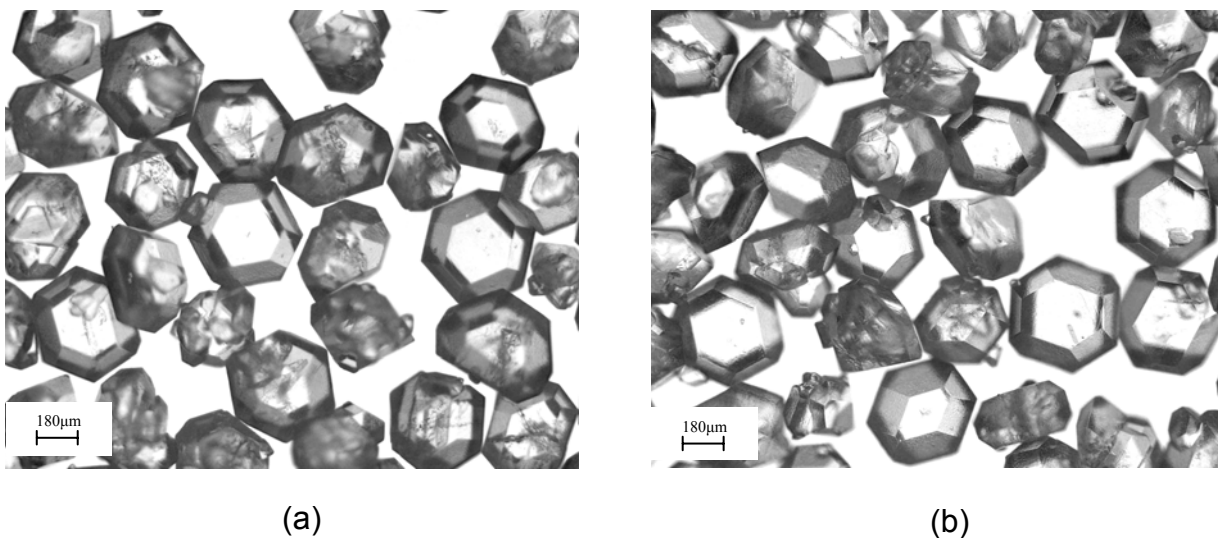
Figure 9. Microscopy images of L-glutamic acid product crystals (α-form):
(a) Run 2, (b) Run 3.
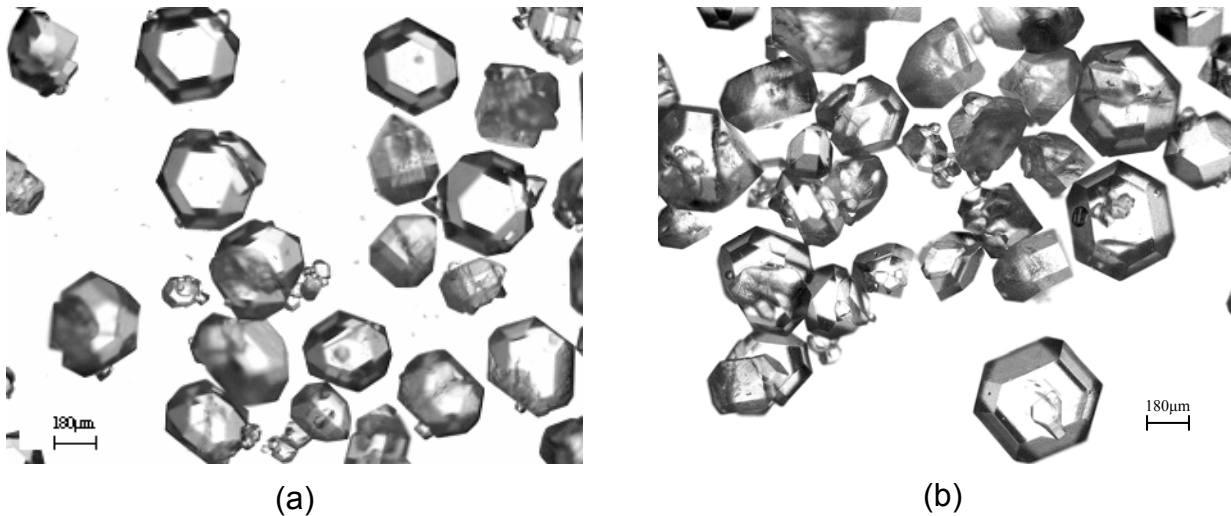
Figure 10. Microscopy images of L-glutamic acid product crystals (α-form) from Run 1: (a) large size variation, (b) agglomeration.

Conclusions

A batch recipe for the selective crystallization with uniform crystal size of metastable polymorph of a monotropic polymorph system, L-glutamic acid in water, was identified through direct design. The solubility curves of both polymorphs were determined using ATR-FTIR spectroscopy, combined with chemometrics. FBRM (laser backscattering) was used to determine the seeded metastable limit. The concentration control strategy, based on in-situ solution concentration measurement and feedback control of the temperature, enabled batch operations at various supersaturation profiles. Undesired α-form secondary nucleation at the metastable limit, as well as β-form secondary nucleation at high temperatures, provided the operating constraints in terms of the maximum allowable supersaturation and operating temperature range, respectively, for the selective crystallization of α-form. Batch crystallization below 40°C at constant relative supersaturation prevented both types of secondary nucleation and was successful in selectively growing large metastable crystals with uniform size. This methodology for the selective growth of metastable crystals may be a practical method applicable to other monotropic polymorph system, because of its direct design approach and flexibility of using different seed loadings or sizes. The metastable limit typically represents the operating boundary to avoid secondary nucleation. However, in a polymorphic system where there are two types of secondary nucleation, it is pertinent to consider the polymorphic transformation behavior, because this dictates additional operating constraints necessary to avoid secondary nucleation of the other form.

Acknowledgements

References

1. Bernstein, J. *Polymorphism in Molecular Crystal*; Clarendon Press: Oxford, 2002.
2. Kitamura, M. *J. of Crystal Growth* **1989**, *96*, 541-546.
3. Ono, T; Kramer, H.; Horst, J.; Jansens, P. *Crystal Growth & Des.* **2004**, *4*, 1161-1167.
4. Ono, T; Horst, J. H.; Jansens, P. J. *Crystal Growth & Design* **2004**, *4(3)*, 465-469.
5. Togkalidou, T; Tung, H. H.; Sun, Y.; Andrews, A. T.; Braatz, R. D. *Ind. Eng. Chem. Res.* **2004**, *43*, 6168-6181.
6. Worlitschek, J.; Mazzotti, M. *Crystal Growth & Design* **2004**, *4*, 891-903.
7. Feng, L. L.; Berglund, K. A. *Crystal Growth & Design* **2002**, *2*, 449-452.
8. Liotta, V.; Sabesan, V. *Org. Process Res. Dev.* **2004**, *8*, 488-494.
9. Gron, H.; Borissova, A.; Roberts, K. J. *Ind. Eng. Chem. Res.* **2003**, *42*, 198-206.
10. Fujiwara, M.; Chow, P.; Ma, D.; Braatz, R. D. *Cryst. Growth & Des.* **2002**, *2*, 363-370.
11. Zhou, G. X.; Fujiwara, M.; Woo, X. Y.; Rusli, E.; Tung, H. H.; Starbuck, C.; Davidson, O.; Ge, Z.; Braatz, R. D. *Crystal Growth & Design* **2006**, *6*, 892-898.
12. Workman, J. J.; Mobley, P.; Kowalski, B.; Bro, R. *Appl. Spec. Rev.* **1996**, *31*, 73-124.
13. Mobley, P. R.; Kowalski, B. R.; Workman, J. J.; Bro, R. *Appl. Spec. Rev.* **1996**, *31*, 347-368.
14. Tahti, T.; Louhi-Kultanen, M.; Palosaari, S. In *Int. Symp. Ind. Cryst., 14th*; Institution of Chemical Engineers: Rugby, UK, 1999; pp 1-9.
15. Barrett, P.; Glennon, B. *Trans. Inst. Chem. Eng.* **2002**, *80*, 799-805.
16. Braatz, R. D. In *The Control Handbook*, Levine, W. S., Ed.; CRC Press Press, Boca Raton, Florida 1995; 215-224.31.
17. Morari, M.; Zafiriou, E. *Robust Process Control*; Prentice Hall: Englewood Cliffs, New Jersey, 1989.
18. Diffracplus Topas (version 3.0) User's Manual, Apr 2005, 2003-2005 AXS Bruker Inc.
19. Lehmann, M. S.; Koetzle, T. F.; Hamilton, W. C. *J. Cryst. Mol. Struct.* **1972**, *2*, 225.
20. Hirayama, N.; Shirahata, K.; Ohashi, Y.; Sasada, Y., *Bull. Chem. Soc. Jpn.* **1980**, *53*, 30.
21. Togkalidou, T; Fujiwara, M; Patel, S.; Braatz, R. D. *J. of Crystal Growth* **2001**, *231*, 534-543.
22. Xie, Y.; Kalivas, J. *Anal. Chim. Acta* **1997**, *348*, 19.
23. Nyvlt, J.; Sohnel. O.; Matuchova, M.; Broul, M. *The Kinetics of Industrial Crystallization*; Elsevier: New York, 1985.
24. Cashell, C.; Sutton, D; Corcoran, D; Hodnett, B. K. *Crystal Growth & Design* **2003**, *3*, 869-872.
25. Ferrari, E. S.; Davey, R. J. *Crystal Growth & Design* **2004**, *4(5)*, 1061-1068.
26. Randolph, A.; Larson, M. A. *Theory of Particulate Processes*; Academic Press: San Diego, CA, 1988.
27. Kitamura, M.; Ishizu. T. *J. of Crystal Growth* **2000**, *209*, 138-145.